

[\[Print Version\]](#)
[\[PubMed Citation\]](#) [\[Related Articles in PubMed\]](#)

TABLE OF CONTENTS

[\[INTRODUCTION\]](#) [\[MATERIALS AND...\]](#) [\[RESULTS\]](#) [\[DISCUSSION\]](#) [\[CONCLUSIONS\]](#) [\[REFERENCES\]](#) [\[TABLES\]](#) [\[FIGURES\]](#)

The Angle Orthodontist: Vol. 74, No. 5, pp. 691–696.

Stiffness in Bending of a Superelastic Ni-Ti Orthodontic Wire as a Function of Cross-Sectional Dimension

Pascal Garrec, DDS;^a Laurence Jordan, DDS^b

ABSTRACT

Superelasticity is a property used in orthodontics to initiate tooth movement in the first stage of orthodontic treatment. It is the aim of all clinicians to accomplish biological tooth movement, which implies the use of low, continuous force and requires archwire with low stiffness. In this study, 15 nickel-titanium archwires with three different cross-sectional dimensions were tested in three-point bending to determine the nature of forces in a loading and unloading cycle. The evolution of stiffness in bending as a function of wire size is discussed. The applied forces or stiffness dependence on cross-sectional size differs from the linear-elastic prediction because of the superelasticity property. We discuss the origin of the nonconventional profile of curves and the nature of reversible large deformation of these alloys. Martensitic transformation is at the origin of nonlinear elasticity. The stiffness decreases with increasing deflection, and this phenomenon is emphasized in the unloading process. The value of stiffness appears to vary with wire size but depends on the ratio of volume of martensitic transformation. During martensitic transformation, the rigidity (elastic modulus) of the alloy is nonconstant. These results and their understanding should allow a different approach of biomechanical considerations, ie, a large-size square wire does not produce necessarily high forces.

KEY WORDS: Hookean elasticity, Nonlinear elasticity, Modulus of elasticity, Martensitic transformation.

Accepted: September 2003. Submitted: June 2003

INTRODUCTION [Return to TOC](#)

Traditionally, the choice of an orthodontic archwire should be based on estimates of forces produced. Biomechanical considerations require forces that are low in magnitude and continuous in nature, ie, archwire with low stiffness. Burstone¹ showed that the orthodontist's choice for a wire size is influenced by its stiffness. Stiffness is directly related to elastic modulus and cross-sectional size and shape.² The past decade has shown that Ni-Ti wires are able to meet the ideal requirements for a fixed archwire appliance and have contributed significantly to the evolution of orthodontic appliance treatment.^{3–5} With these alloys, the stiffness can be reduced without reducing the cross-sectional dimensions in contrast to a conventional alloy.¹

The relationship between the applied force (F) and the deflection (δ) under three-point bending conditions is given by: $F = 48(EI\delta/L^3)$. The forces generated by a deflection in bending are proportional to the deflection, to the modulus of elasticity (E , constant for a conventional alloy), to the moment of inertia of the cross section (I) and inversely proportional (cube power) to the span length between supports (L : interbracket distance). This relationship is useful for comparing the relative values of forces in bending for a few archwires of different alloys and different cross-sectional shapes.^{6,7} A large majority of orthodontists know this, and when using conventional alloys during "leveling" of the teeth (preliminary bracket alignment stage), one must use smaller round cross-section wires (I small) or incorporate complex loop designs (L great) or both to generate small magnitude forces.

However, these requirements suppose that alloys show a linear relationship between stress and strain, which is described by Hooke's law ($\sigma = E\epsilon$) where E , the elastic modulus is constant and does not change with stress and strain.⁷ Shape memory alloys, such as nickel-titanium, are characterized by a reversible phase transformation in solid state, the thermoelastic martensitic transformation, accompanied by a hysteresis. On cooling, the martensitic transformation is governed mainly by the shear of the high-temperature phase unit cell (austenite). A shape change results from this shear, but a finite number of crystallographic equivalent shears lead to a finite number of equivalent variants of the low-temperature phase (martensite). These variants are gathered into self-accommodating groups for a mutual compensation of the deformation, and the final transformed material exhibits no shape change.

The transformation can also be induced by stress. In the case of stress-induced martensitic (SIM) transformation, the property observed is superelasticity. The most favorable variants of martensite, which change in the direction of the external stress, outgrow and are responsible for the large deformation that can be observed. Without the acting stress, the martensite is unstable and specimens recover their original shape after unloading. The reverse transformation causes an unloading plateau. In this case, elasticity has two origins. At small deformations, the alloy shows a linear elasticity (classic Hookean elasticity). At larger deformations, above a given value, the martensitic transformation occurs. The elastic deformation becomes nonlinear.^{7,8}

The aim of this study is to show the evolution of stiffness in bending as a function of cross-sectional dimension. The applied force dependence on cross-sectional size differs from the linear-elastic prediction because of the superelasticity effect.⁹ A conventional three-point bending test is conducted to determine the nature of forces in a loading and unloading cycle. The level of force and stiffness and their dependence on cross-sectional dimension is discussed.

MATERIALS AND METHODS [Return to TOC](#)

A total of 15 wires of a Ni-Ti orthodontic alloy (Thermo NITI®, produced by Ortho-Force, Paris, France) were selected for this study. They represented various cross-sectional dimensions with square shapes available only as preformed arches. Only the straight segments of each preformed arch were tested. The choice of only one manufacturer is necessary because the mechanical properties of Ni-Ti are affected by the chemical composition, process fabrication, and heat treatment of the alloy.^{8,10,11} These parameters are not discussed in this study.

Tests were carried out on five straight square wires of 0.016 inches (0.406 mm), five wires of 0.018 inches (0.457 mm) and five wires of 0.020 inches (0.507 mm). The cross-sectional dimension of each sample was measured (Table 1). The theoretical values of the moment of inertia were calculated (for a real square shape). This value is a geometric quantity that corresponds to the resistance of a particular cross section to bending. For a square beam, the moment of inertia is given by Brantley et al:⁷ $I = a^4/12$, where a is the thickness of the square.

Three-point bending test

To perform bending experiments, a three-point bending test using a free-end beam theory was conducted (Figure 1). All the samples were loaded with the same protocol on a testing machine (GT-Test GmbH Universal testing machine, model 112) with a span at 14 mm.^{3,6} The midportion of the wire segment was then deflected at three mm at the rate of two mm/minute under the pressure from a stylus connected to a 20-N load cell. All the measurements were taken in constant-temperature water. Temperature was regulated by a thermostatic water bath and fixed at $37^\circ\text{C} \pm 0.5^\circ\text{C}$.

Force-deflection diagrams with three cross-sectional dimensions (0.016, 0.018, and 0.020 square inches) were determined from the passive position to a total activation of three mm and then during deactivation to zero.

RESULTS [Return to TOC](#)

The mean values for the cross-sectional dimension of wires are about two standard deviations smaller than their commercial size (Table 1). To facilitate wire placement into the brackets, manufacturers have intentionally smaller cross-section wire dimensions than the nominal dimensions. The moment of inertia increases on the fourth power with the thickness of the wire, ie, the increase is about 46% between the 0.016- and the 0.018-inch wires and about 54% between the 0.018- and the 0.020-inch wires. The bending curves for each cross-sectional dimension are shown in Figure 2. All wires exhibited superelastic behavior,^{7,8,12} but with different loading and unloading levels.

In Figure 3, means are shown graphically at a deflection of 0.15, 0.5, 1, 1.5, 2, and 2.5 mm to observe the evolution of curves when the total bending is achieved at 3 mm. Two plateau regions are visible.

The relationship between the applied force (F) and the deflection (δ) under three-point bending conditions is given by^{7,13}:

$$F = 48 \frac{EI\delta}{L^3} \quad (1)$$

Consequently, the stiffness in bending for an archwire segment of span length L is given by the following. Stiffness in bending is proportional to $\propto EI/L$, where E represents the alloy contribution and I/L the segment geometry contribution to stiffness.

Region of linear elasticity

At 0.15 mm of deflection, the behavior of elasticity is linear and the level of force (Figure 3) or stiffness for each wire is the same at loading and unloading. The slope of the initial and final linear region corresponds obviously to the linear elastic strain. In this small deflection range, Hook's law can be used to describe the stress and strain relationship: $\sigma = E\epsilon$; where E , the elastic modulus is constant, and does not change with stress or strain. For the same deflection, the level of force or stiffness between the 0.016- and the 0.018-inch wires is increased by 44.5% because the increase of the moment of inertia between 0.016-inch wire and the 0.018-inch wire is over 46%. Between the 0.018 and 0.020 inches, the increase is about 42% although the increasing of moment of inertia is about 54% between these two sizes.

Region of nonlinear elasticity

Above a certain force, the elasticity behavior becomes nonlinear. The upper plateau in Figure 2 corresponds to the formation of SIM plates preferentially oriented. On unloading, the reverse transformation occurs and the force-deflection curve follows the lower plateau region. It corresponds to the reverse transformation, and the martensitic phase is gradually transformed back to the austenitic phase. The difference in the magnitude of the forces on the upper plateau at 1.5 mm between archwire 0.016 /0.018 and 0.018/0.020 is about 40%. This difference is clearly less important in the unloading process (Figure 3), where the difference is $\approx 15\%$ than upon loading between the 0.016- and 0.018-inches cross section, but more important than for the 0.018 and 0.020 inches cross section about: $\approx 90\%$. However, the lower plateau region of the 0.020-inch curve is clearly inferior to the loading plateau of 0.016 inch. Whatever the cross-sectional dimension, the stiffness of the material decreases when loading and unloading occurs, but the collapse is more important at the unloading process. The mechanical hysteresis, measured as the difference between the forces of the upper and the lower plateaus, increases with the cross-sectional dimensions (Figure 4).

Moreover, the loading plateau remains constant, but it is associated with a change in the gradient of the SIM, ie, the gradients become steeper with the sample size.^{14,15} This phenomenon is more evident on the diagram of the 0.020-inch sample.

DISCUSSION [Return to TOC](#)

It is of interest to discuss the origin of the nonconventional profile of the loading and unloading curves and thus the origin of reversible deformation of these alloys. Martensitic transformation and deformation have a close relation in various aspects.

At small deformation, the alloy shows a linear elasticity (classic Hookean elasticity) and, similar to conventional alloys, during elastic deformation the atoms move very slightly from their original positions but not to the extent that they take up new positions. When the forces are removed, they return to their original positions. The atomic bonds are just stretched out. The modulus of elasticity is related to the bonding strength between the atoms in a metal or alloy and is constant and independent of wire configuration and nominal wire size.^{7,13} Therefore EI (stiffness in bending) is invariant at loading and unloading process for each cross-sectional size.¹⁶ The stiffness in bending (EI) at the loading and unloading for a deflection at 0.15 mm is calculated when the total bending strain is achieved at 3 mm:

$$-EI_{0.016} = 150 \text{ N}\cdot\text{mm}^2$$

$$-EI_{0.018} = 220 \text{ N}\cdot\text{mm}^2$$

$$-EI_{0.020} = 315 \text{ N}\cdot\text{mm}^2$$

For example, a 0.016 × 0.016-inch stainless-steel wire with $E = 180$ GPa presents a stiffness in bending of $EI = 408$ N·mm² and this value does not change in a bending test. In our results, the value of EI of the three square-size Ni-Ti wire is largely inferior (between 150 and 315 N·mm²).

But we note that the experimental bending stiffness does not increase in step with the cross-sectional dimension (E is constant), especially for the 0.020 × 0.020 inch. In fact, the square shape is not perfect, and the angles are blunt (Figure 5) because these square wires are rolled or sized from round stock. The shape tends to a round configuration. Then, the experimental values of the moment of inertia (I) are smaller than theoretical values. This can make an important contribution to the force delivery.

At large deformation, Ni-Ti alloy wires exhibit superelastic behavior. This type of behavior is also called pseudoelasticity, because there is a complete return to the origin in a loading-unloading cycle, similar to that in a classical linear or nonlinear elasticity. The path of return generates a hysteresis that depends on the amount of dissipated energy during the mechanical cycling. At the beginning of the strain, the alloy is austenitic and stable. At some critical force (F_c), which depends on temperature, the martensitic transformation occurs. Thus, the mechanical behavior of Ni-Ti wires is largely under the dependence of martensitic transformation. The plateau is caused by the ability of martensite to accommodate the applied deflection, by selecting the most favorably oriented variants along the direction of the strain. Each variant is connected with another variant by a twinning plane (intervariant interface) which moves easily upon loading.

At this temperature and without acting stress, this martensite is unstable, and specimens recover their original shape after unloading. The reverse transformation causes an unloading plateau. The original shape recovers completely by reverse transformation accompanied by the reverse movement of the interface between austenite and martensite phases. In this case, the elastic deformation is not a stretching out of bonds but results from a phase transformation with new equilibrium positions of atoms. It is a crystallographic structural change. The growth of most favorable martensitic variants accommodates the applied stress. This phenomenon requires lower energy than the pursuit of the Hookean elasticity and prevents the plastic deformation of the austenite in this temperature and stress range.

To understand the response of Ni-Ti wire, we must take into account the thermodynamic aspect of martensitic transformation. This is not only controlled by chemical free energy, but is also dependent on microstructural factors. Elastic energy is stored during martensite transformation. An equation for a thermodynamic equilibrium between martensite variants and the surrounding austenitic phase can be formulated. $\Delta G_{ch} + \Delta G_{mech} + E_{rev} + E_{fr} = 0$, where $\Delta G_{ch} = G_M - G_A$ is the difference of chemical free energy between austenite and martensite (resistive contribution during loading); ΔG_{mech} is the contribution of the external applied stress; E_{rev} is reversible energy stored (elastic strain energy and variant energy interfaces: A-M, M-M) and E_{fr} is energy dissipated by friction due to the movement of interfaces and formation of defects. The above equation means that part of the driving force (E_{rev}) is stored in the material through a nondissipate process during the forward transformation. Then, elastic energy stored in the alloy during the forward martensite transformation and frictional energy, lost because of movement of interfaces, are both controlling factors in the profile of curves.

The increasing loading plateau and gradient as a function of cross-sectional dimension corresponds to increasing elastic strain energy, ie, the ratio of martensitic transformation and frictional energy transformation is higher. Therefore, the applied stress required to transform austenite to martensite does not stay constant and gradually increases with the volume fraction of transformed martensite.

The unloading process is controlled by the reverse transformation and is dominated by the stored energy. The stored elastic energy (E_{rev}) obviously contributes to the driving force (with ΔG_{ch}) and assists the reverse transformation. The position of the variants in the deformed state is not stable without stress, and thus, there is this driving force causing them to return to their original positions during unloading. Consequently, the unloading plateau (mechanical hysteresis) is reduced compared with the level of the loading plateau.

The main clinical interest of this hysteresis is that the force delivered to the periodontal structures is lower than the force necessary to activate the wire. For the same maximum deformation, the volume of SIM increases with the cross-sectional dimension. Therefore, the area of the mechanical hysteresis increases. The stored elastic energy increases with the same proportion and will facilitate the reverse transformation. The stiffness in bending is not constant, and it decreases with deflection. The collapse is more important at the unloading, ie, even in the bigger size, the 0.020 × 0.020 inch, the stiffness in bending (calculated at 1.5, 2, and 2.5 mm of deflection) is about eight times inferior (± 50 N·mm²) to those of stainless steel in an unloading process. During martensitic transformation (forward and reverse), it is not the relative concentration of the two phases in the alloy that will determine the resultant stiffness of the wire. Rather, it is the process of martensitic transformation, the stiffness of the material collapses and the modulus of elasticity dramatically decreases. In this case, the term "pseudomodulus of elasticity" is certainly more correct.

CONCLUSIONS [Return to TOC](#)

It is important that estimations of the forces produced by superelastic Ni-Ti be based on a perfect understanding of the physics and especially the value of the wire stiffness involved. In this manner, this parameter can be controlled with better efficiency.

In our investigation, the influence of different cross-sectional dimensions of a Ni-Ti archwire (larger cross-section) was studied. Our results show that the factor of primary importance is the martensitic transformation. Indeed, during martensitic transformation, the rigidity of the alloy collapses and the modulus of elasticity decreases. This collapse largely dominates the increasing moment of inertia. Thus, the theoretical prediction of Hooke's law in the loading or unloading plateau is not established. The stiffness in bending is not directly linked with the cross-sectional size, when a superelasticity process exists. Consequently, the biomechanical objectives of an orthodontic treatment could be achieved with higher cross-sectional dimension wires that exhibit martensitic transformation. Satisfactory adaptation of the wire in the bracket slot must occur, allowing optimal physiologic tooth displacement. This behavior gives to the clinician an opportunity to vary the traditional argument and to achieve optimal performances of the archwire throughout all stages of orthodontic treatment.

ACKNOWLEDGMENTS

The authors are grateful to Prof Richard Portier and Dr Frédéric Prima for their support.

REFERENCES [Return to TOC](#)

1. Burstone CJ. Variable-modulus orthodontics. *Am J Orthod*. 1981; 80:1–15. [\[PubMed Citation\]](#)
2. Oltjen JM, Manville GDJ, Ghosh J, Nanda RS, Currier GF. Stiffness-deflection behavior of selected orthodontic wires. *Angle Orthod*. 1997; 67:3209–218. [\[PubMed Citation\]](#)
3. Miura F, Mogi M, Ohura Y, Hamanaka H. The super-elastic property of the Japanese NiTi alloy wire for use in orthodontics. *Am J Orthod Dentofacial Orthop*. 1986; 90:1–10. [\[PubMed Citation\]](#)
4. Hirokazu Nakano, Kazuro Satoh, Robert Norris, Tomoaki Jin, Tetsuya Kamegai, Fujiro Ishikawa, Hirofumi Katsura. Mechanical properties of several nickel-titanium alloy wires in three-point bending tests. *Am J Orthod Dentofacial Orthop*. 1999; 115:390–394. [\[PubMed Citation\]](#)
5. Burstone CJ, Quin B, Morton JY. Chinese NiTi wire: a new orthodontic alloy. *Am J Orthod*. 1985; 87:445–452. [\[PubMed Citation\]](#)
6. Gurgel JA, Kerr S, Powers JM, Lecrone V. Force-deflection properties of superelastic nickel-titanium archwires. *Am J Orthod Dentofacial Orthop*. 2001; 120:378–382. [\[PubMed Citation\]](#)

7. Brantley WA, Eliades T, Litsky AS. Mechanics and mechanical testing of orthodontic materials. In: *Orthodontic Materials*. Stuttgart: Thieme, eds; 2001:28–32.
8. Guénin G. Alliages à mémoire de forme. *Tech ingénieur*. 1986; 10:1–11.
9. Muraviev SE, Ospanova GB, Shlyakhova MY. Estimation of force produced by nickel-titanium superelastic archwires at large deflections. *Am J Orthod Dentofacial Orthop*. 2001; 119:604–609. [[PubMed Citation](#)]
10. Jordan L, Masse M, Collier JY, Bouquet G. Effects of thermal and thermomechanical cycling on the phase transformations in NiTi and Ni-Ti-Co shape memory alloys. *J Alloys Compounds*. 1994;211–212, 204–207.
11. Thayer AT, Bagby MD, Moore RN, DeAngelis RJ. X-ray diffraction of nitinol orthodontic arch wires. *Am J Orthod Dentofacial Orthop*. 1995; 107:604 [[PubMed Citation](#)]
12. Norme AFNOR. Alliages à mémoire de forme: Vocabulaire et mesures. (Indice de classement A 51-080.), edited by annotation, française de normalisation, Paris. April 1991.
13. Dorlot JM, Bailon JP, Masounave J. Les méthodes de caractérisation des matériaux. In: *Des Matériaux*. Montréal: Editions de l'Ecole Polytechnique de Montréal; 1986:13–15.
14. Van Humbeeck J, Stalmans R, Chandrasekaran M, Delaey L. On the stability of shape memory alloys. In: Duerig TW, Melton KN, Stöckel D, Wayman CM, *Engineering Aspects of Shape Memory Alloys*. London: Butterworth-Heinemann; 1990:96–105.
15. Morgan NB, Friend CM. A review of shape memory stability in NiTi alloys. *J Phys IV*. 2001; 11:325–332.
16. Kusy RP, Shish AM. Geometric and material parameters of a nickel-titanium and a beta titanium orthodontic arch wire alloy. *Dent Mater*. 1987; 3:207–217. [[PubMed Citation](#)]
17. Duerig TW, Zadno R. An engineer's perspective of pseudoelasticity. In: Duerig TW, Melton KN, Stöckel D, Wayman CM *Engineering Aspects of Shape Memory Alloys*. London: Butterworth-Heinemann, eds; 1990:369–393.
18. Otsuka K, Ren X. Martensitic transformations in nonferrous shape memory alloys. *Mater Sci Eng*. 1999A; 273–275:89–105.
19. Tamura I, Wayman CM. *Martensitic Transformations and Mechanical Effects*. In: *Martinsite*. USA Olson GB, Owen WS, eds. 1992:227–242.

TABLES [Return to TOC](#)

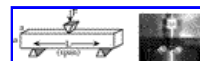
TABLE 1. Means, Standard Deviations and Moment of Inertia of Sample Size

Nominal Wire Size Square (inch)	Mean (Standard Deviation) (inch)	Moment of Inertia I (10^{-4} mm^4)	Variation of Moment of Inertia I (%)
0.016 × 0.016	0.015984 (± 0.0001647)	22.64	↓ +46 ↓ +54
0.018 × 0.018	0.017583 (± 0.0003992)	33.15	
0.020 × 0.020	0.019590 (± 0.0002202)	51.09	

TABLE 2. Theoretical Values of Moment of Inertia (I) as a Function of Shape

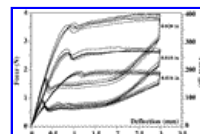
Nominal Wire Size (inch)	I Square Shape (10^{-4} mm^4)	I Round Shape (10^{-4} mm^4)
0.016	22.64	13.34
0.018	33.15	19.52
0.020	51.09	30.09

FIGURES [Return to TOC](#)



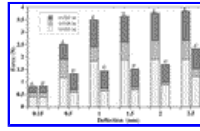
[Click on thumbnail for full-sized image.](#)

FIGURE 1. Schematic drawing of the three-point bending, apparatus, and the deflected wire



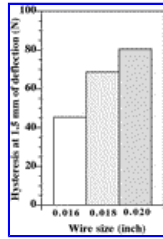
[Click on thumbnail for full-sized image.](#)

FIGURE 2. Force/deflection curves for the 0.016, 0.018- and 0.020-inch wire samples at 37°C



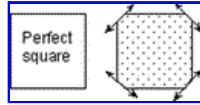
Click on thumbnail for full-sized image.

FIGURE 3. Mean of forces of the 0.016-, 0.018-, and 0.020-inch wire samples at different deflections (L = load ; U = unload)



Click on thumbnail for full-sized image.

FIGURE 4. Evolution of mechanical hysteresis at 1.5 mm of deflection



Click on thumbnail for full-sized image.

FIGURE 5. Section view of a "blunt" square wire

^aPrivate practice. Department of Orthodontics and College of Dentistry, University Denis Diderot of Paris, France. Laboratory of Structural Metallurgy, ENSCP, Paris, France

^bAssistant Professor, Department of Dental Materials, College of Dentistry, University Denis Diderot of Paris, France. Laboratory of Structural Metallurgy, ENSCP, Paris, France

Corresponding author: Dr. Pascal Garrec, 115, Avenue du Maine, 75014 Paris, France.(E-mail: pascal.garrec@wanadoo.fr)